Journal of Animal & Plant Sciences, 32(3): 2022, Page: 694-704
ISSN (print): 1018-7081; ISSN (online): 2309-8694
http://doi.org/10.36899/JAPS.2022.3.0471

=DIFFERENTIALLY EXPRESSED GENE PROFILE AND RELEVANT PATHWAYS IN THE PLACENTA OF PREGNANT MICE IN RESPONSE TO MATERNAL THYROID HORMONE ADMINISTRATION

W. M. Chen, L. X. Li, L. L. Niu and T. Zhong*

Farm Animal Genetic Resources Exploration and Innovation Key Laboratory of Sichuan Province, College of Animal Science and Technology, Sichuan Agricultural University, Chengdu 611130, China
*Corresponding Author's email: zhongtao@sicau.edu.cn

ABSTRACT

Thyroid hormone has pleiotropic regulatory effects on growth, development, and metabolism. It also regulates cell proliferation, differentiation, and apoptosis. In the present study, differentially expressed genes (DEG) and their related pathways involved in TH regulation during gestation were identified in the placenta tissues of high thyroid-induced mice by RNA sequencing. The levels of TSH, FT_3, and FT_4 in blood showed an increasing tendency in the high thyroid-induced mice with intragastric administration of 0.250 or 0.500 $\mu g \cdot \mu L^{-1}$ L-T_4, respectively. Compared to CG9d mice, one DEG and 10 DEGs were identified in the LG9d and HG9d groups, respectively. There were 32 DEGs identified between the LG9d and HG9d, 22 of which were up-regulated DEGs and 10 were down-regulated. Several GO annotations and signaling pathways were associated with embryonic development and TH synthesis and metabolism, including the Wnt signaling pathway and the TH signaling pathway. The expressions of nine randomly selected DEGs were re-quantified by quantitative real-time PCR (qPCR) and showed a consistent tendency with the results of RNA-sequencing, which suggests that reliable data are obtained in the transcriptome assay. These findings provide insights into the mechanism of the dynamic regulation of the TH balance during pregnancy in mammals.

Key words: mice, thyroid hormone, transcriptome, DEG, signaling pathway

Published first online October 20. 2021 Published final May 30. 2022

INTRODUCTION

Thyroid hormone (TH) is a general term of 3, 5, 3 ', 5 '- tetraiodothyronine (thyroxine, T_4) and 3, 5', 3 - triiodothyronine (T_3) compounds containing iodine atoms (Carvalho and Dupuy, 2017). The thyroid is the only source of T_4, but most T_3 is produced by deiodination of the outer ring of T_4 by deiodinase type 3 (*DIO3*), which is highly expressed in the placenta (van der Spek *et al*., 2017). Most actions of TH are initiated by binding with T3 to nuclear receptors encoded by the *THRA* and *THRB* genes. It is widely accepted that T_4 predominantly acts as a prohormone for the active hormone T_3 (Visser, 2016). The hypothalamic-pituitary-thyroid (HPT) axis of the fetus begins to develop around five weeks of gestation and does not secrete TH until the 18th week of gestation (Stanley *et al*., 2001; Landers and Richard, 2017).

TH plays an important role in organ development and metabolic homeostasis in mammals, as TH is a key regulator of growth, development, and metabolism in almost all tissues, mainly regulating cell proliferation, differentiation, and apoptosis (Mullur *et al*., 2014). TH disorders, either excess (Hyperthyroidism) or insufficiency (hypothyroidism) of TH during development, could also result in structural brain abnormalities (Alkemade, 2015). In fetal rats, the consequences of maternal thyroid dysfunction led to adverse alterations in neuronal development, synaptogenesis, and myelination in the brain. In pregnancy mice, high levels of TH can increase the craniofacial abnormalities in offspring (Durham *et al*., 2017), while a lack of TH may lead to neurological disorders, such as the maternal decline in their descendants. Maternal hyperthyroidism could result in many maternal and fetal adverse events, such as pre-eclampsia, miscarriage, stillbirth, preterm birth, and intrauterine growth restriction (Fetene *et al*., 2017). Furthermore, maternal thyroid dysfunction may relate to pregnancy complications and increase disease incidence in fetuses (Laurberg and Andersen, 2015). Gestational hypothyroidism was found to induce transgenerational effects on glucose metabolism in mice offspring, which may affect predisposition to type 2 diabetes development in response to metabolic stress (Kemkem *et al*., 2020).

In the TH signaling pathway, many DEGs, such as *SLC16A2*, *CCND1*, *RXRA*, and PKCα, have been successfully identified by the transcriptomic analysis (Liu *et al*., 2015; Ochsner and McKenna, 2020; Stauffer *et al*., 2021). *SLC16A2* has 12 transmembrane domains and transports the active form of thyroid hormone, T_3, and its precursor T_4. Moreover, it has been suggested that *SLC16A2* cooperates with *Slco1c1* or *Slc7a8* in the brains of mice, which improves the possibility of transporter combinations controlling additional developmental

functions (Sharlin *et al*., 2018). T3-bound nuclear thyroid hormone receptor β1 (TRβ1) inhibited the β-catenin-dependent transactivation of the *CCND1* promoter through the Tcf/Lef-1 site. T_4 significantly increased the interaction between β-catenin and the promoter region of *CCND1* (Lee *et al*., 2018). Overexpression of PKCα could induce cardiomyocyte markers to suppress the expression of thyroid hormone-responsive genes, including SERCA2 and α- and β-MHC. After treatment with T_3 for 4 h, the level of PKCα in the nuclear and cellular compartments decreases significantly (Kenessey *et al*., 2006).

TH secreted by the maternal in the first trimester mainly plays an important role in the growth and development of the fetus through the placental barrier, while the underlying molecular mechanism is still unclear. Therefore, we performed the study to identify the candidate genes and pathways involved in TH metabolism in high-thyroid-induced mice by RNA-sequencing.

MATERIALS AND METHODS

Animals and TH treatment: Experimental animals involved in this study were approved by the Institutional Animal Care and Use Committee at the College of Animal Science and Technology, Sichuan Agricultural University, China. Sixty-five 6-week-old female and nine male KM mice were purchased from the Chengdu Dossy Laboratory Animal Co., Ltd (Sichuan, China). Mice were raised separately by gender and housed at 20 ± 2 °C under a 12 h/ 12 h light/dark cycle with free access to food and water for one-week acclimatization.

Seven-week-old female mice were injected intraperitoneally with 10 units of PMSG in a volume of 300 μL of normal saline and mated after 48 hours. Pregnant mice checked by the presence of a vaginal plug were blindly divided into three groups: one control group (CG, receiving gavage of normal saline, n = 10) and two TH gavage groups, receiving 0.250 $\mu g \cdot \mu L^{-1}$ (LG, n = 14), or 0.500 $\mu g \cdot \mu L^{-1}$ (HG, n = 20) of L-thyroxine (L-T_4, Sigma-Aldrich, Germany), respectively. Each female mouse was kept in a single cage and administered a volume of 80 μL of L-T_4 daily.

Sample collection and serum TH levels measurement: The mice in the three groups were killed on gestation days 9 and 18 (GD9 and GD18). Blood samples were collected by eye enucleation with coagulation-promoting tubes. Serum levels of FT_3, FT_4, and Thyroid-stimulating hormone (TSH) were determined using a CHEMCLIN®600. Automatic Chemiluminescence Instrument (Beijing Kemei Biotechnology Co., Ltd) at the Rehabilitation Hospital in Sichuan Province. Placental tissues were obtained by surgery and frozen in liquid nitrogen for further analysis.

RNA isolation and transcriptome sequencing: Total RNA was isolated from placenta tissues using the RNAiso Plus reagent (Takara, Dalian, China). The concentration of RNA was determined using a NanoDrop ND-2000 spectrophotometer (Thermo Scientific, Wilmington, DE, USA). RNA was evaluated on the basis of the RNA integrity number using an Agilent 2100 Bioanalyzer (Agilent Technologies, Santa Clara, CA, USA). cDNA was synthesized using the SuperScript™ II Reverse Transcriptase kit (Invitrogen, Carlsbad, CA, USA) with random hexamer primers. Samples were purified using AMPure XP beads (Beckman Coulter, Brea, CA, USA) to remove chemical contaminants and short RNA less than 200 nt in length. Subsequently, blunt-end cDNA was 3'-adenylated ligated to sequencing adapters. cDNA was finitely amplified by using a Primer Cocktail (Illumina) and purified with paramagnetic beads. The Qubit RNA Assay kit and a Qubit 2.0 Fluorescence Reader (Life Technologies, Carlsbad, CA, USA) were used for quality control and quantitative validation. Finally, the libraries were subjected to 50 bp single-end read sequencing using an Illumina HiSeq™ 2500 sequencing system (Illumina).

Quality control and data analyses: Raw data were evaluated to remove low-quality reads and adapter sequences using the FASTX-Tool kit (http://hannonlab.cshl.edu/fastx_toolkit/index.html).

Clean reads were mapped with the mouse genome GRCm38 assembly using HISAT2 (http://www.ccb.jhu.edu/software/hisat/). The amount of sequencing data and the length of the transcripts were normalized to reflect the transcript expression level. FPKM (Fragments per kilobase of transcript per million mapped fragments) was used as an index to measure the transcript expression level. DEGs were identified by FDR correction and the fold-change method using DESeq2_EBSeq, according to a corrected P-value ≤ 0.05 and a fold-change value ≥ 1.0. Functional enrichment analysis was used to determine the enriched Gene Ontology of the DEGs in the mouse placenta. A P value (< 0.05) indicated significant GO term enrichment among the DEGs. Pathway analysis was used to map the DEGs to Kyoto Encyclopedia of Genes and Genomes (KEGG) pathways.

Sequencing results validated by qPCR: Six upregulated genes and three downregulated genes were selected to verify the results of RNA sequencing. The qPCR primers were designed by the Primer Premier 5.0 software (Table 1). qPCR was performed in a volume of 15 μL including 7.5 μL 2X SYBR Premix Ex Taq II (Takara), 0.6 μL cDNA, and 0.3 μM primers and carried on the CFX96 Connect system (Bio-Rad, Richmond, CA, USA). PCR conditions were as follows: 95 ° C for 30 s, then 39 cycles of 95 ° C for 10 s, and Tm° C for 30 s. Each sample was quantified in triplicate. The specificity of the

product was confirmed by the melting curve analysis. The *GAPDH* gene was used as the reference gene to quantify mRNA expression using the $2^{-\Delta\Delta Ct}$ method.

RESULTS

Effect of L-T_4 gavage on serum TH levels in pregnant mice: As shown in Fig. 1, the levels of TSH, FT_3, and FT_4 in the blood of pregnant mice following L-T_4 gavage gradually increased. Furthermore, when the pregnant mice were treated with L-T_4 at the same concentration, the TSH, FT_3, and FT_4 levels of the mice sacrificed on the 18th day of gestation were higher than those sacrificed on the 9th day of gestation.

Preliminary analyses of RNA data in TH mice: A total of 344,298,583 clean reads were obtained from 12 samples after removing adapter sequences and low-quality reads, and 91.16% to 96.43% of the clean reads were mapped to the mouse reference genome (GRCm38). In these samples, 7,023,630,104 to 11,353,594,796 clean bases were obtained. The clean reads were used for statistical analysis of base content and the base mass distribution. The GC content of these samples was above 50% and the Q30 reached 93%, indicating that the base composition of the sequencing data was good and could be used for subsequent analysis (Table 2).

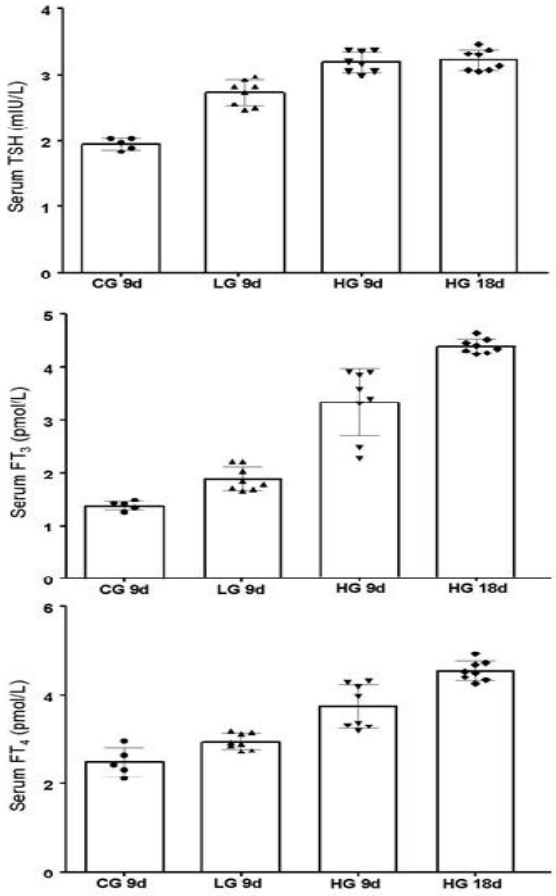

Figure 1. Concentrations of TSH, FT_3 and FT_4 in the blood of pregnant mice in different dose groups.

Table 1. Primer information of qPCR used in this study.

Gene	Accession No.	Primer sequence (5'-3')	Size (bp)	Tm (°C)
Ncoa2	NM_001302702.1	CAGAAATACGAGGCGATGC GATGAGGGAAGAGTTGGTC	137	55.6
RCAN1	NM_019466.4	CGTGGTCTCGCTCGTTCT GCCCTGGTCTCACTTTCG	185	58
Tbc1d4	NM_001081278.2	CAGTAGCATCAGGCAGTTA CTTCTTATGGGTCACGATC	136	55.6
SLC16A10	NM_028247.4	CAGCCGTCACTGGTCATT GAGGTCGGTAGGTAAAGC	208	58
Pik3cb	NM_029094.3	GTCTTGGATCGACTGGCTAA GAGGCGTTTCTGGATTGC	199	59.3
Rxra	NM_001290481.1	GCACCGGGAAGGGTAAAT TTCAGCCGCCTGGTAAGC	167	59.3
Ccnd1	NM_007631.2	CGCCCTCCGTATCTTACT ACCTCCTCTTCGCACTTC	105	59.3
Atp1a3	XM_021166048.1	GACAAACTGGTCAACGAA CTGCCAGGATGACAAAGT	100	53.5
Prkca	NM_011101.3	CGACCACTCGGGCTATCA GGCTCCCTTGCTGTAAAT	110	59.6
GAPDH	NM_008084.3	GGTGAAGGTCGGTGTGAACG CTCGCTCCTGGAAGATGGTG	233	59.5

Table 2. Summary of mRNA sequencing results in this study.

Sample	Clean Reads	Mapped Reads	Clean Bases	Q30 (%)	GC Content (%)
CG9d-1	26,991,619	52,025,951 (96.37%)	8,053,851,882	94.30%	50.42%
CG9d-2	23,550,576	45,260,796 (96.09%)	7,023,630,104	94.53%	50.87%
CG9d-3	27,253,708	52,559,188 (96.43%)	8,110,640,690	94.30%	50.65%
CG9d-4	30,256,178	56,574,257 (93.49%)	9,048,273,580	93.71%	51.07%
HG9d-1	23,598,054	43,766,963 (92.73%)	7,046,061,644	93.02%	51.57%
HG9d -2	26,552,943	50,476,279 (95.05%)	7,922,243,450	93.15%	50.33%
HG9d-3	23,739,992	43,284,766 (91.16%)	7,080,817,122	93.55%	51.99%
HG9d-4	28,636,405	54,156,582 (94.56%)	8,572,264,470	94.46%	51.71%
HG18d-1	37,912,698	72,054,748 (95.03%)	11,353,594,796	94.87%	51.31%
HG18d-2	33,353,480	63,003,480 (94.45%)	9,984,314,924	94.63%	51.55%
HG18d-3	29,953,146	56,562,091 (94.42%)	8,966,153,278	94.67%	51.80%
HG18d-4	32,499,784	61,418,371 (94.49%)	9,731,961,948	94.68%	51.83%
Total	344,298,583	651,143,472	102,893,807,888		

Identification of DEGs following L-T_4 gavage: A total of 7877 DEGs were identified in the four groups (Fig. 2a), including HG9d vs CG, CG vs LG9d, LG9d vs HG9d, and HG9d vs HG18d. There was one gene, *Hr*, common to both the HG9d vs CG and the CG vs LG9d pairs, identified to be linked to thyroid hormone receptors. There were 7 genes common to both the HG9d vs CG and the HG9d vs HG18d pairs, 2 genes common to the CG vs HG9d and the LG9d vs HG9d pairs, 24 genes common to the LG9d vs HG9d and the HG9d vs HG18d pairs. To better survey the dynamic regulation mechanism of TH balance during pregnancy, it was important to identify DEGs in placenta tissues treated with different concentrations of TH. Gene expression between the control group (CG) and experimental groups (LG9d, HG9d, and HG18d) was compared and visualized in a volcano plot. There was one significant upregulated DEG in the CG and LG9d groups (Fig. 2b). Ten significant genes were differentially expressed in the CG and HG9d groups, including 3 upregulated genes and 7 downregulated genes (Fig. 2c). 32 significant genes were differentially expressed in the LG9d and HG9d groups, including 22 upregulated genes and 10 downregulated genes (Fig. 2d).

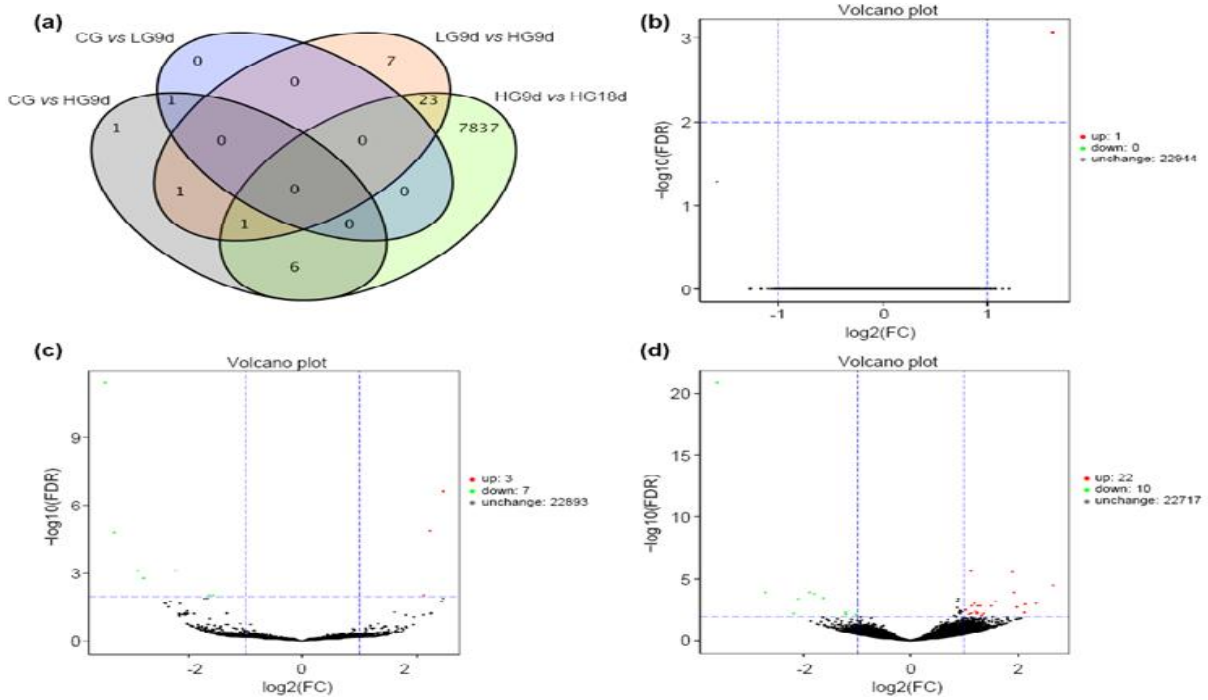

Figure 2. The Venn diagram summarizes the number of DEGs found in this study (a). Volcano plot of DEGs in the CG9d and HG9d groups (b). Volcano plots of DEGs in the CG9d and LG9d groups (c). Volcano plots of DEGs in the LG9d and HG9d groups (d).

Enrichment of DEGs and their relevance to TH metabolism: The obtained DEGs were classified and annotated according to the cell component, molecular function, and biological process categories of the GO database (Fig. 3). The pathways showing the DEGs enrichment in the molecular function category were related to the protein binding, zinc ion binding, ATP binding, and histone deacetylase binding activity terms (Supplementary Fig. 1). The pathways enriched in the cell component classifications included cytoplasm, nucleolus, mitochondrion, and cytoplasmic parts. In addition to cell components and molecular functions, GO terms for multiple biological processes were related to the functions of DEGs. The protein autophosphorylation, transport, heterodimerizations, and phosphate-containing compound metabolic processes were enriched by DEGs.

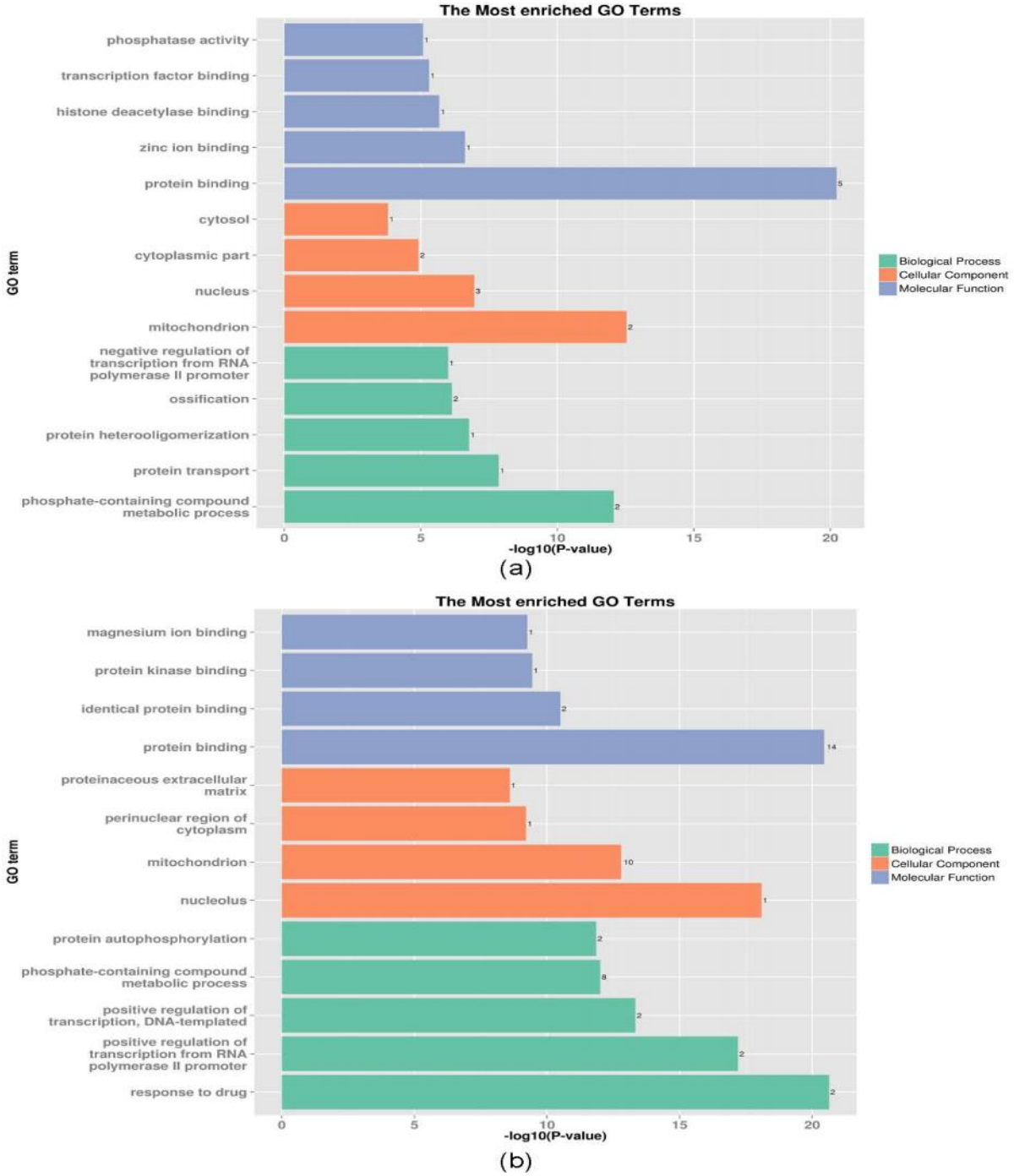

Figure 3. GO analysis for DEGs between the CG9d and HG9d groups (a). GO analysis for DEGs between the LG9d and HG9d groups (b).

To better understand the functions of the DEGs, the genes were mapped to the KEGG database for analysis (Fig. 4). The results showed that among the 41 pathways, differentially expressed genes were mainly enriched in pathways related to cancers, the Hippo signaling pathway, oxidative phosphorylation, proteoglycans in cancer, the Wnt signaling pathway, the TH signaling pathway and so on. Analysis of these pathways suggested that thyroid hormones may enter the blood circulation of the embryo through the placental barrier, thereby regulating the normal development of the embryo. Nine DEGs, *Ccnd1*, *Atp1a3*, *Med30*, *Prkca*, *Rcan1*, *Med12l*, *Pik3cb*, and *Rxra*, which may be related to embryonic growth and development, were screened from the above pathways.

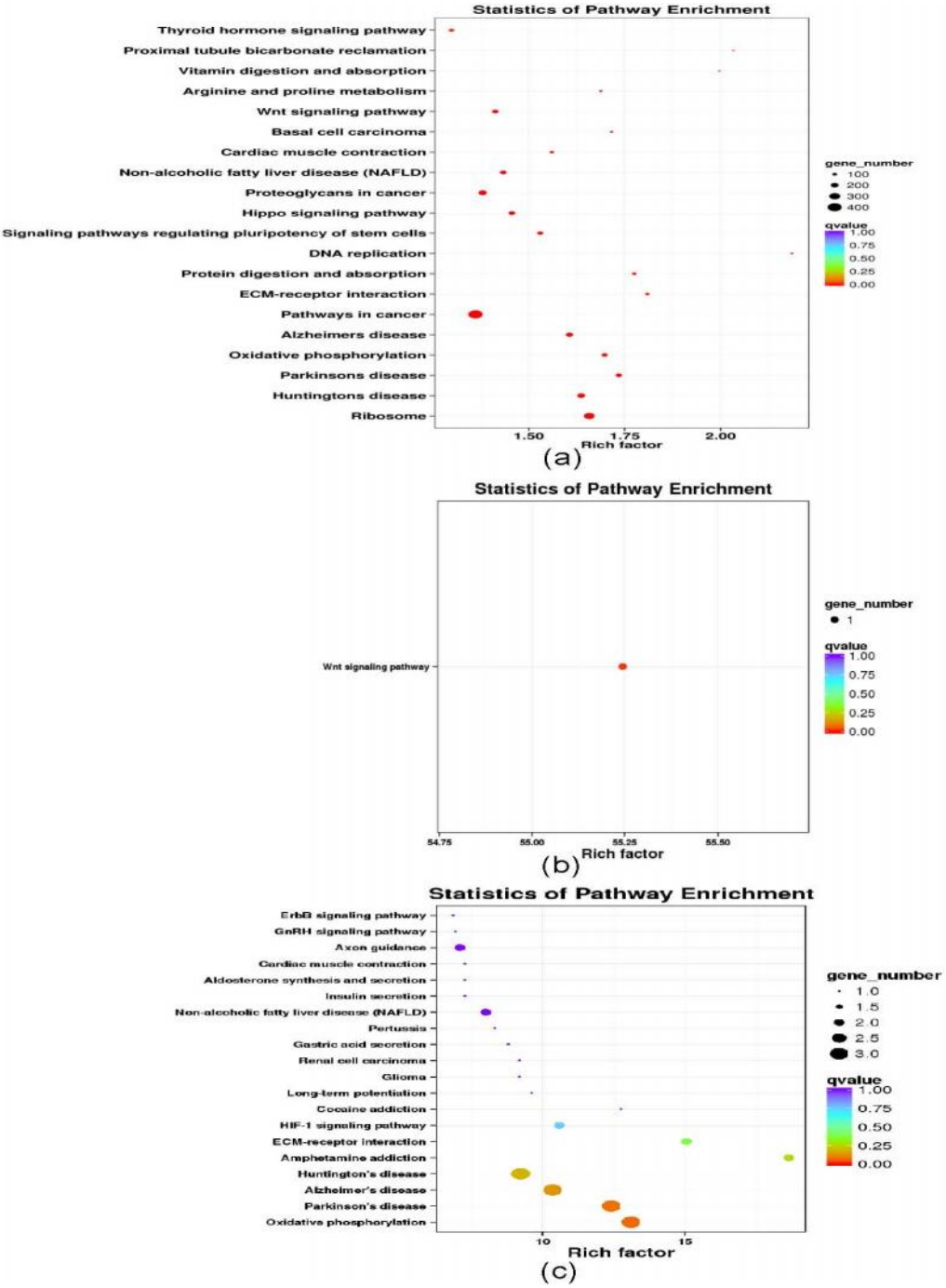

Figure 4. Enriched pathway between the DEGs from the HG9d and HG18d groups (a), CG and HG9d groups (b), LG9d and HG9d groups (c).

Signal pathway analyses: The transcriptome results showed that TH was involved in 15 pathways, which included the following: TH signaling pathway (ko04919), TH synthesis (ko04918), TH transmembrane transporter activity (GO: 0015349), TH transport (GO: 0070327), cellular response to TH stimulus (GO: 0097067), TH metabolic process (GO: 0042403), thyroid gland development (GO: 0030878), positive regulation of TH generation (GO: 2000611) and TH receptor coactivator activity (GO: 0030375). We focused on the TH signaling pathway. Although the major form of TH in the blood is T_4, it is converted to the more active hormone T3. T3 binds to nuclear thyroid hormone receptors (TRs), which function as ligand-dependent transcription factors and control the expression of target genes. Alpha(v)beta (3)-integrin has distinct binding sites for T_3 and T_4 in the plasma membrane. One binding site binds only T_3 and activates the phosphatidylinositol 3-kinase (PI3K) pathway. The other binding site binds both T_3 and T_4 and activates the ERK1/2 MAP kinase pathway.

Verification of DEGs from RNA sequencing results: To verify the expression profile of DEGs revealed in the RNA-Seq analyses, qPCR was performed to quantify the expression of the nine selected DEGs. As shown in Fig. 5, the expression levels of *Ncoa2*, *Rcan1*, *Tbc1d4*, *SLC16A10*, *Pik3cb*, and *Rxra* were increased in the HG18d group, while the expression levels of Ccnd1, *Atp1a3*, and *Prkca* were decreased. These results were consistent with the tendencies of the RNA sequencing results, suggesting that the results of transcriptome sequencing are reliable.

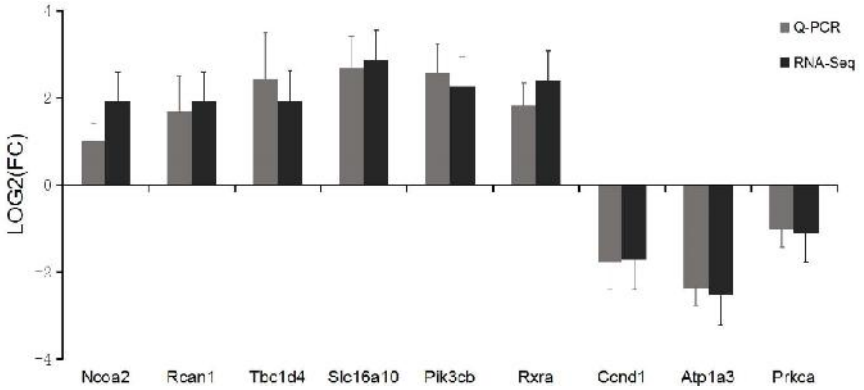

Figure 5. Validation of the nine selected DGEs by qPCR.

DISCUSSION

In the present study, the levels of TSH, FT_3, and FT_4 in the blood showed a tendency of rising. We also quantified the *DIO3* mRNA expression in the placenta by qPCR, which represented that the *DIO3* expression in the placenta increased following the increase of L-T_4 concentration in pregnant mice (Supplementary Fig. 1). These findings indicated that the experimental results were consistent with the fact that a large amount of *DIO2* converts T_4 into T_3 in the cells of some tissues (van der Spek *et al*., 2017). Meanwhile, we speculate that the increase of TSH may be caused by the destruction of the hypothalamic-pituitary-thyroid axis, and T_4 and T_3 are affected by the negative feedback to control the secretion of TSH, which cannot maintain the physiological level of the main hormones in the HPT axis.

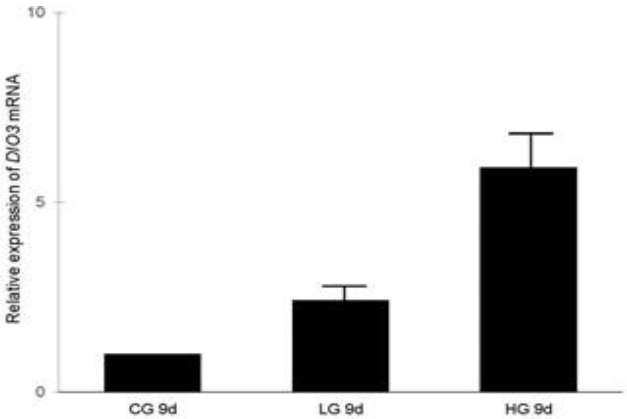

Supplementary Fig. 1. Expression of DIO3 in placenta (9d).

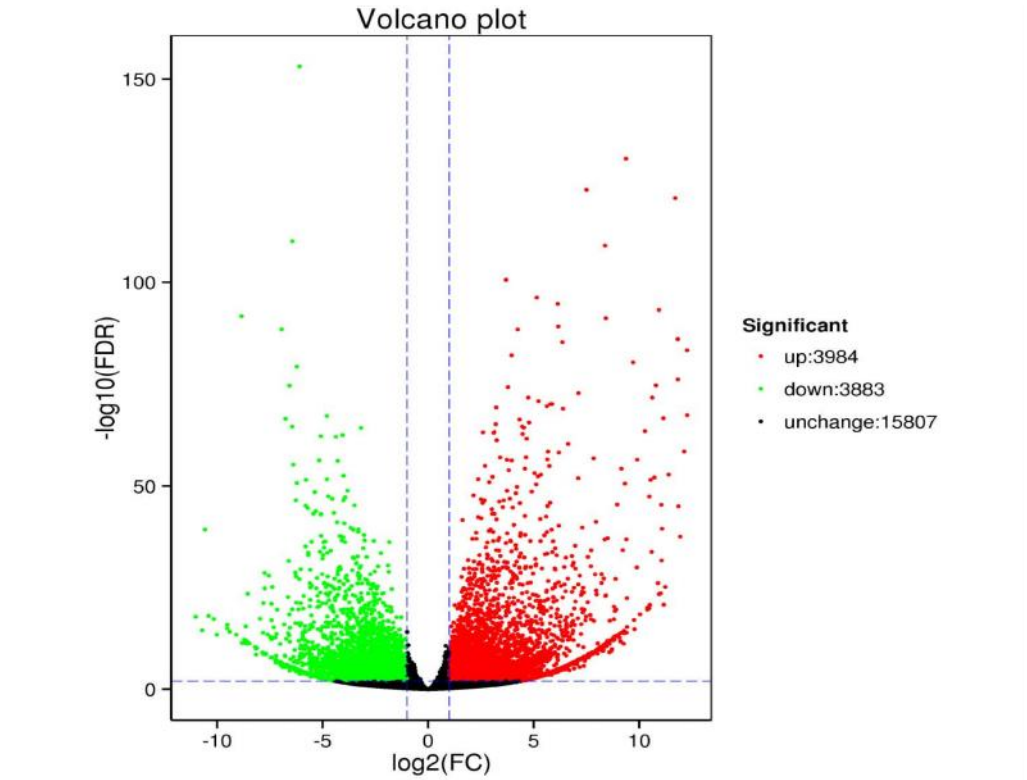

(a)

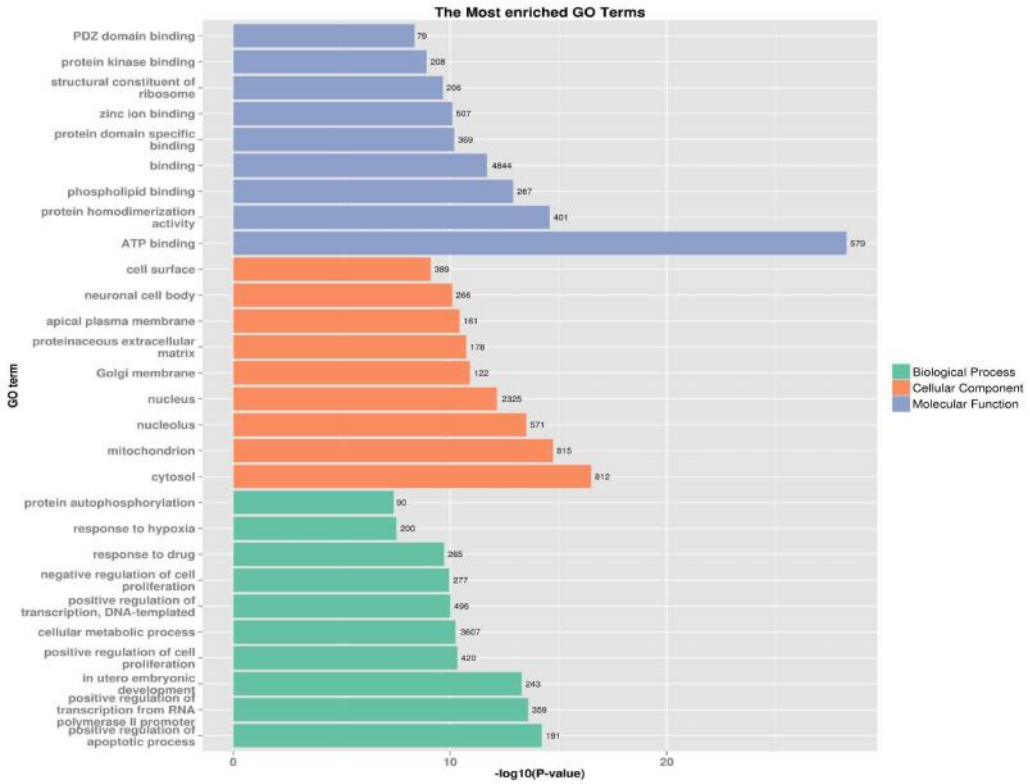

(b)

Supplementary Fig. 2. Volcano plots of DEGs in the HG9 and HG18d groups (a). GO analysis for DEGs between the HG9d and HG18d groups (b).

In this study, seven significant DEGs (*Ccnd1*, *Rcan1*, *Rxra*, *Gata1*, *Ctsb*, *Pax8*, and *Col1a2*) associated with fetal growth and development were identified. The previous study has been shown that *Pax8* was considered to be the marker gene of thyroid differentiation (Filippone *et al*., 2014). *Pax8* is mainly expressed in the kidney and thyroid. It is the main gene involved in thyroid development and differentiation (de Cristofaro *et al*., 2012). In the early stages of thyroid development, *Pax8* is necessary for the survival of a cell during migration until it reaches its final location (Di Palma *et al*., 2013). In addition, *Pax8* may mediate heart development in mice through cellular senescence to compensate for cell apoptosis during heart development (Wu *et al*., 2016). Compared with the CG group, the *Rxra* and *Rcan1* genes were upregulated in the HG18d group, while *Prkca* genes were downregulated. The protein encoded by the *Rxra* gene is a member of the transcriptional regulatory superfamily of steroids and thyroid hormone receptors (Kolsch *et al*., 2009). It could form the permissive heterodimers to regulate nutrient metabolism, or generate the non-permissive heterodimers as the TH receptor. *Rcan1* was mainly involved in the inhibition of calcium phosphatase and the regulation of mitochondrial function. Short-term induction of *Rcan1* expression is generally thought to be protected through the expression of pro-survival genes in a variety of cell types, which is mediated by the NFAT transcription pathway in many cases (Peiris and Keating, 2018).

Ccnd1 encodes a cyclin that controls key transitions in the cell cycle and its expression and cellular localization are typically transformed in human tumor cells. *Ccnd1* forms complexes with CDK4 or CDK6 and acts as a regulatory subunit. Its activity is required for G1/S conversion, and *Ccnd1* also interacts with the tumor suppressor pRB1 (Cao *et al*., 2017). As a zinc-finger transcription factor, *Gata1* is critical in the differentiation, proliferation, and apoptosis of red blood cells and megakaryocytes (Peters *et al*., 2015). In addition, *Gata1* is a key regulator of vascular endothelial growth factor (VEGF) expression and tumor angiogenesis (Zhang *et al*., 2016). *Ctsb* is responsible for driving proteolytic degradation in the lysosome and in the extracellular environment. *Ctsb* cleaves the calcium channel MCON1/TRPML1 in the lysosome, maintaining inhibition of the transcription factor TFEB and decreasing the expression of lysosome and autophagosomes (Man and Kanneganti, 2016). In the present study, the above-mentioned DEGs were identified as the candidate genes associated with TH metabolism in mice. However, it is crucial to point that those DEGs could be limited by the small sample size in our study. Therefore, the identification of candidate genes using a larger sample size could generate more reliable results.

TH plays an important role in the development of fetal neuro-intelligence, bone, and the cardiovascular system (Springer *et al*., 2017). Especially in the TH administration mice in later pregnancy, many DEGs were identified between the HG9d and HG18d groups. Among them, several DEGs that affect fetal growth and development were identified after GO and KEGG analysis (Supplementary Fig. 2). The Wnt signaling pathway is critical for tissue development and homeostasis by regulating endogenous stem cells. The Wnt signaling involves many basic processes necessary for embryonic development and normal adult tissue homeostasis (Duchartre *et al*., 2016). The Wnt signaling is pleiotropic for different pathways involved in vascular smooth muscle plasticity and cardiac, renal, and neurophysiology (Abou Ziki and Mani, 2017). Studies have shown that the Wnt signaling pathway is significantly involved in the pathogenesis of cardiac fibrosis, and this pathway may play a key role in the activation and proliferation of cardiac fibroblasts (Tao *et al*., 2016). It is also involved in the proliferation, differentiation, and migration of cells, especially during the development of the nervous system.

Conclusion: In this study, we identified expression changes in candidate DEGs related to TH metabolism in mouse placentas. GO annotations and signaling pathways were associated with embryonic development, TH synthesis and metabolism, including the Wnt signaling pathway and TH signaling pathway. The findings suggest that the DEGs may play a certain role in fetal vital activities by regulating TH metabolism.

Authors' Contributions: T. Z. and L. N. participated in Conceptualization, Data curation, and Review editing, W. C. and L. L. participated in Sample collection, Methodology, Analyzing data, and Writing-original draft, T. Z. participated in Funding acquisition, Project administration, and Supervision. All authors have read and agreed to the published version of the manuscript.

Disclosure statement: The authors have declared that no competing interests.

Acknowledgments: The study was funded by the undergraduate innovation and entrepreneurship training program of Sichuan Province (201710626093).

Data Availability Statement: The RNA-seq data were deposited to the NCBI Sequence Read Archive (SRA) database (SUB5871649).

REFERENCES

Abou Ziki, M. D. and A. Mani (2017). Wnt signaling, a novel pathway regulating blood pressure? State of the art review. Atherosclerosis 262: 171-178.

Alkemade, A (2015). Thyroid hormone and the developing hypothalamus. Front. Neuroanat. 9: 15.

Cao, L., P. Zhang, J. Li, and M. Wu (2017). LAST, a c-Myc-inducible long noncoding RNA, cooperates with CNBP to promote CCND1 mRNA stability in human cells. Elife 6: e30433.

Carvalho, D. P. and C. Dupuy (2017). Thyroid hormone biosynthesis and release. Mol. Cell Endocrinol. 458: 6-15.

de Cristofaro, T., T. Di Palma, I. Fichera., V. Lucci., L. Parrillo, M. De Felice, and M. Zannini (2012). An essential role for Pax8 in the transcriptional regulation of cadherin-16 in thyroid cells. Mol. Endocrinol. 26: 67-78.

Di Palma, T., M. G. Filippone, G. M. Pierantoni, A. Fusco, S. Soddu, and M. Zannini (2013). Pax8 has a critical role in epithelial cell survival and proliferation. Cell Death Dis. 4: e729.

Duchartre, Y., Y. M. Kim, and M. Kahn (2016). The Wnt signaling pathway in cancer. Crit. Rev. Oncol. Hematol. 99: 141-149.

Durham, E., R. N. Howie, T. Parsons, G. Bennfors, L. Black, S. M. Weinberg, M. Elsalanty, J. C. Yu, and J. J. Cray (2017). Thyroxine exposure effects on the cranial base. Calcif. Tissue Int. 101: 300-311.

Fetene, D. M., K. S. Betts, and R. Alati (2017). MECHANISMS IN ENDOCRINOLOGY: Maternal thyroid dysfunction during pregnancy and behavioural and psychiatric disorders of children: a systematic review. Eur. J. Endocrinol. 177: R261-273.

Filippone, M. G., T. Di. Palma, V. Lucci, and M. Zannini (2014). Pax8 modulates the expression of Wnt4 that is necessary for the maintenance of the epithelial phenotype of thyroid cells. BMC Mol. Biol. 15: 21.

Kemkem, Y., D. Nasteska, A. de Bray, P. Bargi-Souza, R. A.Peliciari-Garcia, A. Guillou, P. Mollard, D. J. Hodson, and M. Schaeffer (2020). Maternal hypothyroidism in mice influences glucose metabolism in adult offspring. Diabetologia 63: 1822-1835.

Kenessey, A., E. A. Sullivan, and K. Ojamaa (2006). Nuclear localization of protein kinase C-alpha induces thyroid hormone receptor-alpha1 expression in the cardiomyocyte. Am. J. Physiol. Heart Circ. Physiol. 290: H381-389.

Kolsch, H., D. Lutjohann, F. Jessen, J. Popp, F. Hentschel, P. Kelemen, S. Friedrichs, T. A. Maier, and R. Heun (2009). RXRA gene variations influence Alzheimer's disease risk and cholesterol metabolism. J. Cell Mol. Med. 13: 589-598.

Landers, K. and K. Richard (2017). Traversing barriers - How thyroid hormones pass placental, blood-brain and blood-cerebrospinal fluid barriers. Mol. Cell Endocrinol. 458: 22-28.

Laurberg, P. and S. L. Andersen (2015). Graves'-Basedow disease in pregnancy. New trends in the management and guidance to reduce the risk of birth defects caused by antithyroid drugs. Nuklearmedizin 54: 106-111.

Lee, Y.S., Y. T. Chin, Y. J. Shih, A. W. Nana, Y. R. Chen, H. C. Wu, Y. S. H.Yang, and H. Y. Lin (2018). Thyroid hormone promotes β-catenin activation and cell proliferation in colorectal cancer. Horm. Cancer 9: 156-165.

Liu, J. L., T. S. Wang, M. Zhao, Y. Peng, and Y. S. Fu (2015). A Transcriptomic Study of Maternal Thyroid Adaptation to Pregnancy in Rats. Int. J. Mol. Sci. 16: 27339-27349.

Man, S. M. and T. D. Kanneganti (2016). Regulation of lysosomal dynamics and autophagy by CTSB/cathepsin B. Autophagy 12: 2504-2505.

Mullur, R., Y. Y. Liu, and G. A. Brent (2014). Thyroid hormone regulation of metabolism. Physiol. Rev. 94: 355-382.

Ochsner, S. A. and N. J. McKenna (2020). No Dataset Left Behind: Mechanistic Insights into Thyroid Receptor Signaling Through Transcriptomic Consensome Meta-Analysis. Thyroid 30: 621-639.

Peiris, H. and D. J.Keating (2018). The neuronal and endocrine roles of RCAN1 in health and disease. Clin. Exp. Pharmacol. Physiol. 45: 377-383.

Peters, I., N. Dubrowinskaja, H. Tezval, M. W. Kramer, C. A. von Klot, J. Hennenlotter, A. Stenzl, R. Scherer, M. A. Kuczyk, and J. Serth (2015). Decreased mRNA expression of GATA1 and GATA2 is associated with tumor aggressiveness and poor outcome in clear cell renal cell carcinoma. Target Oncol. 10: 267-275.

Sharlin, D.S., L. Ng, and F. Verrey (2018). Deafness and loss of cochlear hair cells in the absence of thyroid hormone transporters Slc16a2 (Mct8) and Slc16a10 (Mct10). Sci. Rep. 8: 4403.

Springer, D., J. Jiskra, Z. Limanova, T. Zima, and E. Potlukova (2017). Thyroid in pregnancy: From physiology to screening. Crit. Rev. Clin. Lab Sci. 54: 102-116.

Stanley, E. L., R. Hume, T. J. Visser, and M. W. Coughtrie (2001). Differential expression of sulfotransferase enzymes involved in thyroid hormone metabolism during human placental development. J Clin. Endocrinol. Metab. 86: 5944-5955.

Stauffer, E., P. Weber, T. Heider, C. Dalke, A. Blutke, A. Walch, G. Burgstaller, N. Brix, K. Lauber, H. Zitzelsberger, K. Unger, and M. Selmansberger (2021). Transcriptomic landscape of radiation-induced murine thyroid proliferative lesions. Endocr. Relat. Cancer 28: 213-224.

Tao, H., J. J.Yang, K. H. Shi, and J. Li (2016). Wnt signaling pathway in cardiac fibrosis: New

insights and directions. Metabolism 65: 30-40.

van der Spek, A. H., E. Fliers, and A. Boelen (2017). The classic pathways of thyroid hormone metabolism. Mol. Cell Endocrinol. 458: 29-38.

Visser, T. J (2016). Thyroid hormone transport across the placenta. Ann. Endocrinol. (Paris) 77: 680-683.

Wu, Y., X. Zhou, X. Huang, Q. Xia, Z. Chen, X. Zhang, D. Yang, and Y. J. Geng (2016). Pax8 plays a pivotal role in regulation of cardiomyocyte growth and senescence. J. Cell Mol. Med. 20: 644-654.

Zhang, Y., J. Liu, J. Lin, L. Zhou, Y. Song, B. Wei, X. Luo, Z. Chen, Y. Chen, J. Xiong, X. Xu, L. Ding, and Q.Ye (2016). The transcription factor GATA1 and the histone methyltransferase SET7 interact to promote VEGF-mediated angiogenesis and tumor growth and predict clinical outcome of breast cancer. Oncotarget 7: 9859-9875.